HHS Public Access

Author manuscript

Neurobiol Aging. Author manuscript; available in PMC 2023 July 01.

Published in final edited form as:

Neurobiol Aging. 2022 July ; 115: 60–69. doi:10.1016/j.neurobiolaging.2022.03.015.

Differences between multimodal brain-age and chronological-age are linked to telomere shortening

Junhong Yu[1,*], **Madhu Mathi Kanchi**[2,3], **Iris Rawtaer**[4], **Lei Feng**[5], **Alan Prem Kumar**[2,6], **Ee-Heok Kua**[5], **Rathi Mahendran**[5,*], **Alzheimer's Disease Neuroimaging Initiative**[a]

[1]Psychology, School of Social Sciences, National Technological University, 48 Nanyang Avenue, Singapore 639798.

[2]Department of Pharmacology, Yong Loo Lin School of Medicine, National University of Singapore, 14 Medical Drive, Singapore 119559

[3]Department of Genome Sciences, The John Curtin School of Medical Research, The Australian National University, Canberra, ACT 2601

[4]Department of Psychological Medicine, Sengkang General Hospital, 110 Sengkang E way, Singapore 544886

[5]Department of Psychological Medicine, Mind Science Centre, Yong Loo Lin School of Medicine, National University of Singapore, 10 Medical Drive, Singapore 117597

[6]NUS Center for Cancer Research, Yong Loo Lin School of Medicine, National University of Singapore, MD3, 16 Medical Drive. Level 4, #04-01, Singapore 117600.

Abstract

Telomere shortening is theorized to accelerate biological aging, however, this has not been tested in the brain and cognitive contexts. We used machine learning age-prediction models to determine brain/cognitive age and quantified the degree of accelerated aging as the discrepancy between brain/cognitive and chronological ages (i.e. age gap). We hypothesized these age gaps

[*]Correspondence should be addressed to: Dr. Junhong Yu, Assistant Professor, Psychology, School of Social Sciences, National Technological University, Singapore. Address: 48 Nanyang Avenue, Singapore 639798. junhong.yu@ntu.edu.sg Or Dr. Rathi Mahendran, Senior Consultant and Associate Professor, Department of Psychological Medicine, Yong Loo Lin School of Medicine, National University of Singapore, NUHS Tower Block, Level 9, 1E Kent Ridge Road, Singapore 119228, pcmrathi@nus.edu.sg, Tel: (65) 67723893, Fax: (65) 67772191.

Yu Junhong: Writing - Original Draft, Conceptualization, Methodology, Software, Formal analysis, Visualization. Madhu Mathi Kanchi: Writing - Review & Editing, Investigation Iris Rawtaer: Writing - Review & Editing, Lei Feng: Writing - Review & Editing, Alan Prem Kumar: Writing - Review & Editing, Resources. Kua-Ee Heok: Resources, Writing - Review & Editing, Project administration, Funding acquisition Rathi Mahendran: Resources, Writing - Review & Editing, Project administration, Funding acquisition

for the Alzheimer's Disease Neuroimaging Initiative

[a]Data used in preparation of this article were obtained from the Alzheimer's Disease Neuroimaging Initiative (ADNI) database (adni.loni.usc.edu). As such, the investigators within the ADNI contributed to the design and implementation of ADNI and/or provided data but did not participate in analysis or writing of this report. A complete listing of ADNI investigators can be found at: http://adni.loni.usc.edu/wpcontent/uploads/how_to_apply/ADNI_Acknowledgement_List.pdf

Declarations of interest

none

are associated with telomere length (TL). Using healthy participants from the ADNI-3 cohort (N=196, Age_{mean}=70.7), we trained age-prediction models using four modalities of brain features and cognitive scores, as well as a 'stacked' model combining all brain modalities. Then, these six age-prediction models were applied to an independent sample diagnosed with mild cognitive impairment (N=91, Age_{mean}=71.3) to determine, for each subject, the model-specific predicted age and age gap. TL was most strongly associated with age gaps from the resting-state functional connectivity model after controlling for confounding variables. Overall, telomere shortening was significantly related to older brain but not cognitive age gaps. In particular, functional relative to structural brain-age gaps, were more strongly implicated in telomere shortening.

Keywords

Brain-age; cognitive-age; telomere; resting-state functional connectivity; structural connectivity; subcortical gray matter; cortical thickness

1. Introduction

Telomeres are nucleoprotein structures that protect the ends of chromosomes (Turner et al., 2019; Zhang et al., 2016). They maintain genomic stability by protecting the genomic DNA from degradation (Giardini et al., 2014). Telomere length (TL) is often proposed as a marker of cellular aging because telomeres are shortened with aging as a result of incomplete DNA replication. The rate at which TL is shortened varies across individuals and is largely attributed to the exposure to DNA replication, oxidative and inflammatory stressors. Thus, TL reflects the cumulative lifetime exposure to these stressors. Naturally, shorter TLs are linked to poor health and increased mortality (Njajou et al., 2009).

Previous research has documented various adverse brain-related outcomes associated with telomere shortening. In terms of gray matter (GM) volume, studies found shorter telomeres linked to significant atrophy, mostly in the subcortical/limbic regions (Jacobs et al., 2014; King et al., 2014; Powell et al., 2018). Findings from brain connectivity studies similarly revealed limbic-related network disruptions in the structural and resting-state functional connectivity modalities (Staffaroni et al., 2018; Yu et al., 2020). However, the accumulated evidence is less consistent on the relationship between TL and cognitive functions. Although some studies showed that shorter TLs were associated with worse cognitive functions (Hägg et al., 2017; Leibel et al., 2020; Ma et al., 2019), many other studies reported the opposite (Lee et al., 2017; Mahoney et al., 2019; Yu et al., 2020) or null associations (Brown et al., 2018; Zhan et al., 2018).

While it has been theorized and shown that telomere shortening is associated with accelerated aging in general (Njajou et al., 2009), this theory has not been tested specifically in the context of brain-aging. It is unclear if the telomere-shortening associated changes in the brain and cognitive domains described earlier reflect accelerated brain-aging, or perhaps age-irrelevant pathophysiological processes. These brain- and cognitive-related changes need not be specific to aging; they can arise as a result of non-aging-related factors. For instance, similar limbic abnormalities were found to be present in youths diagnosed with depression (Redlich et al., 2018) and those with significant psychopathic tendencies (Blair

and Zhang, 2020). Likewise, cognitive impairments were also commonly present in young adults diagnosed with mood disorders (Castaneda et al., 2008).

With the advent of brain-age machine learning prediction methods (Cole and Franke, 2017), we can now put an 'age' to an individual's brain according to certain brain characteristics such as gray matter atrophy, cortical thickness, and connectivity between different regions, and then relate this brain age to variations in TL. If one's brain-age is older than his/her chronological age, we can infer that the individual is undergoing accelerated brain aging. This difference between brain-age and chronological age have been commonly referred to as the brain age gap. Across the lifespan, accelerated brain aging is linked to other types of aging such as biological aging, older facial appearance (Elliott, et al., 2021), and cognitive decline. Concerning the latter, older adults diagnosed with neurocognitive disorders such as mild cognitive impairment (MCI) and Alzheimer's disease (AD) were found to possess significantly 'older' brain age gaps as compared to their cognitively normal counterparts (Löwe et al., 2016).

One major limitation with many previous brain-age prediction studies was that they trained their age-prediction models solely on one class of brain features (e.g., GM or cortical surface) and this may not adequately capture the effects of aging in the brain. Furthermore, it has been shown that the combination of cortical and functional connectivity features produced more accurate brain-age predictions than either type of features alone (Liem et al., 2017). Hence, in the current study, our brain-age prediction models were derived from four different modalities— resting-state functional connectivity (rsFC), structural connectivity (SC), cortical thickness (CT), and subcortical GM volume (subGM). This will enable us to exploit a far more comprehensive range of age-related brain features in estimating brain age.

In the current study, we used the Alzheimer's Disease Neuroimaging Initiative (ADNI) dataset to train multimodal brain-age prediction models. We also trained a cognitive-age prediction model in a similar manner. These models were then applied to an independent sample of older adults with MCI to predict their brain- and cognitive-age. Then, we assessed the associations between TL and the brain/cognitive-chronological age gaps. We hypothesized that 'older' brain- and cognitive-age gaps were associated with shorter TL. We chose to study individuals with MCI since they are likely to present with lower cognitive scores and atypical brain features such as disrupted white matter microstructure (Yu et al., 2017), resting-state connectivity (Badhwar et al., 2017), and significant GM atrophy (Minkova et al., 2017), as compared to cognitively normal individuals. These abnormalities will translate into larger or more variable brain/cognitive-chronological age deviations, thus making it easier to detect significant associations between brain/cognitive-chronological age gaps and TL.

2. Methods

2.1 Participants

Two independent groups of participants were used in this study. The first group consisted of participants from the Alzheimer's Disease Neuroimaging Initiative (ADNI). Their data were downloaded from the ADNI's database (adni.loni.usc.edu). The ADNI was launched

in 2003 as a public-private partnership, led by Principal Investigator Michael W. Weiner, MD. The primary goal of ADNI has been to test whether serial magnetic resonance imaging (MRI), positron emission tomography (PET), other biological markers, and clinical and neuropsychological assessment can be combined to measure the progression of MCI and early AD. For up-to-date information, see www.adni-info.org.

A total of 196 participants from the ADNI-3 baseline database who 1) were not diagnosed with dementia or MCI, 2) have valid cognitive test (described in the subsequent section) data, 3) have valid MRI data, and 4) had their rsfMRI scans acquired using single-band EPI sequences were included. Those with rsfMRI scans acquired using only multiband EPI sequences were excluded. These different EPI sequences are not compatible with each other. Most of the participants had at least an rsfMRI scan acquired using a single-band EPI sequence, as opposed to the multiband EPI sequence. Details regarding the criteria for dementia and MCI used in the ADNI are available at https://adni.loni.usc.edu/wp-content/uploads/2008/07/adni2-procedures-manual.pdf. Ethical approval for the ADNI study was obtained by the ADNI investigators.

The second group consisted of participants recruited in Singapore (SG dataset) for two different intervention studies (Yu et al., 2021a, 2021b) with identical neurocognitive assessments and MRI acquisition protocols. For the current study, the baseline data from both interventions were combined. These participants were recruited from the same community. The inclusion criteria were 1) aged between 60 and 85 (inclusive), 2) met the criteria for mild cognitive impairment (MCI), 3) able to travel to the intervention venue independently, 4) not presenting with any current neurological conditions, 5) not suffering from any terminal illness and 6) not participating in another interventional study. These participants were diagnosed with MCI (Petersen, 2004) by a consensus panel. Details on the operationalization of the MCI diagnosis are reported in their parent intervention studies. Written informed consent was obtained from these participants prior to their participation. Ethical approvals for both intervention studies were granted by the National University of Singapore Institutional Review Board.

The SG dataset consisted of 121 participants in total. Among the 121 participants, MRI data were acquired from 95. Two subject's MRI data were discarded due to obvious MRI abnormalities and another two were discarded due to excessive head motion during their rsfMRI scans. The remaining 91 participants with valid MRI data were included in the age-prediction analyses. They consisted of 15 single-domain amnestic, 44 single-domain nonamnestic, 12 multiple-domain amnestic and 20 multiple-domain non-amnestic MCI cases Among scanned sample, 82 had valid TL measurements and were included in the analyses involving TL. The demographic characteristics of the two groups of participants are presented in table 1.

2.2 Cognitive measures

We included all available cognitive measures which are similar or at least comparable in SG and ADNI datasets. These tests were administered either in English or Mandarin in the SG sample, depending on the participant's preference.

The Color Trails Test (CTT) (D'Elia and Satz, 1996) and Trail Making Test (TMT) (Reitan, 1992) were used in the SG and ADNI samples, respectively, to assess divided attention, visual scanning, and processing speed. Both tests are highly similar; the CTT was thought to be a culturally neutral analog of the TMT (D'Elia and Satz, 1996). Although previous studies have observed the non-equivalence of performance in the second parts of the TMT and CTT, these differences were largely attributed to the effect of native language (Lee et al., 2000; Lee & Chan, 2000). To this end, the CTT may be more appropriate for use in the SG sample, which consisted of both English and Mandarin-speaking participants. Each of these tests consisted of two parts. In the first, participants connected a series of numbers that were printed within circles, sequentially from 1 to 25. Subsequently, in the second part participants alternated between choosing numbers in either pink or yellow circles while similarly connecting the numbers from 1 to 25 for the CTT. Whereas in the TMT, participants alternated between numbers and alphabet, in sequential order (i.e., 1-A-2-B-3-C, etc.). Three outcome measures were used in this study— the completion times for both parts, as well as the interference effect (i.e., [part 2 – part 1]/part 1). The CTT has demonstrated good reliability, as well as concurrent and construct validity in the local Singaporean context (Chew et al., 2020).

The Rey Auditory Verbal Learning Test (RAVLT; Rey, 1941) was used to assess verbal immediate and delayed recall, as well as recognition memory. Participants were given a list of 15 unrelated words (list A) to learn and immediately recall aloud over five learning trials (Immediate Recall). Subsequently, an interference list of 15 unrelated words (list B) was presented only once for the participants to learn and recall immediately, following which, the participants were instructed to recall aloud the words from list A. Approximately 30 minutes later, they were again asked to recall aloud the words from list A (Delayed Recall). Finally, they were given a list of 50 words, comprising of list A, list B, and 20 new distractor words, from which to identify the original 15 words (Recognition). The RAVLT have been previously reported to be valid, responsive and reliable in the local context (Shen et al., 2014).

The MMSE (Folstein et al., 1975) was used to assess for general cognitive ability. It was scored on a 30-point scale and consisted of 24 items assessing orientation, attention, calculation, recall, and language. A validated local adaptation (Feng et al., 2012) of the MMSE was administered in the SG sample. In this local adaptation, some of the word stimuli were replaced with more locally and culturally relevant ones.

For these measures, higher scores corresponded to better performance, except for the CTT/TMT outcomes, in which longer completion times and larger interference were associated with worse performance.

2.3 Telomere measurements

Whole blood samples were collected in the morning, upon fasting overnight into vacutainer tubes containing EDTA (lavender colour) and are stored immediately in a mini-fridge (4 °C) and transported within 12 hours of collection into the tubes. Subsequently, they are then centrifuged (2000rpm) for 10 minutes and their plasma is collected into 1.8ml cryo vials for further analysis of stress-related markers. The whole blood cells were then subjected to

genomic DNA extraction using QIA amp DNA blood mini kit (cat.no. 51104) according to the manufacturer's protocol and stored at −80°C. Telomere length was measured using a non-radioactive chemiluminescent telomere length assay kit (Telo TAGGG assay kit, Sigma Aldrich; cat.no.12 209 136 001) to visualize the telomeric DNA repeat sequence TTAAGGG from blood samples. Telomere length measurement involves the digestion of 1ug of DNA using Hinf I /Rsa I enzymes at 37°C for 2 hours, and run on 0.8% agarose gel. DNA smears were transferred on to the nylon membrane (Amersham Hybond TM-XL) overnight. Transferred DNA fragments are hybridized to a digoxigenin (DIG) labelled probe to validate the telomeric repeats developed by CDP-Star, which is a digoxigenin substrate to capture the imaging by X-ray film. Telomere length was measured by the location of bands based on molecular weight standard, in the white blood cell DNA. Average telomere length is measured between 100 base pairs to 20 kilo base pairs. These TL measurements were measured in 15 batches; TLs from each respective batch were normalised by using the positive control run in each batch. The image processing, detection of DNA smears and, subsequently measurement of telomere length were carried out using TeloTool (Gohring et al., 2014) in MATLAB, as described in a previous study (Rane et al., 2015). The inter-assay coefficients of variability was calculated to be 26.9%

2.4 MRI acquisition

Participants in the SG dataset were scanned in a 3-T Siemens Tim Trio scanner at the Clinical Imaging Research Center, Singapore. T1-weighted images were acquired using an MPRAGE protocol (TE=1.90s; TR=2.30s; TI=900ms; 256 × 256 matrix; 192 sagittal slices; in-plane resolution=1mm; slice thickness=1mm). For the resting-state fMRI, 310 EPI volumes were acquired. (TR = 2.30s; TE = 25ms; 48 axial slices; matrix = 64 × 64; in-plane resolution=3mm; slice thickness=3mm). During the resting-state fMRI scan, subjects were instructed to close their eyes and remain as motionless as possible. Diffusion-weighted images were acquired using a multi-shell High Angular Resolution Diffusion Imaging (HARDI) protocol, consisting of 14 b0 images, 60 diffusion directions at $b = 1000\ s/mm^2$ and 60 diffusion directions at $b = 3000\ s/mm^2$ (TE=111ms; TR=6.7s; 84 × 84 matrix, 48 axial slices, in-plane resolution=3mm; slice thickness=3mm). Details regarding the MRI acquisition protocol in the ADNI sample are available at http://adni.loni.usc.edu/wpcontent/uploads/2017/07/ADNI3-MRI-protocols.pdf

2.5 Image processing

The MRI data from both datasets were preprocessed using the same pipeline. T1-weighted images were preprocessed using the CAT12 as implemented in SPM12 within MATLAB. First, the T1-weighted images were corrected for bias–field inhomogeneities. Then, they were segmented into grey matter (GM), white matter (WM), and cerebrospinal fluid (CSF). These GM and WM images were used to estimate spatial normalization deformation fields using the high dimensional Diffeomorphic Anatomic Registration Through Exponentiated Lie Algebra (DARTEL) warping algorithm (Ashburner, 2007) which were applied to segmented images and subsequently modulated. These modulated images were then visually inspected. Finally, the 'volume estimation for ROI' writing option was used to extract region-of-interest (ROI) values from the Neuromorphometrics atlas (http://

www.neuromorphometrics.com/). All subcortical GM regions, excluding the cerebellum, were entered into the subsequent analyses.

Estimation of CT and the central surface was carried out using the projection- based thickness method (Dahnke et al., 2013), which consisted of topology correction (Yotter, Dahnke, Thompson, & Gaser, 2011), spherical mapping, and spherical registration (Yotter, Thompson, & Gaser, 2011). After obtaining the segmented images, WM distance was estimated and the local maxima were projected to other GM voxels using a neighbor relationship described by the WM distance (Dahnke et al., 2013). The 'surface thickness and thickness estimation for ROI' writing option was used to extract ROI values from the Destrieux atlas (Destrieux et al., 2010). All of these ROI values were subsequently entered into the analyses.

The resting-state functional MRI data were preprocessed using data processing assistant for resting-state fMRI (DPARSF), advanced version (Yan, Wang, Zuo, & Zang, 2016). Briefly, the first 10 volumes were removed to allow for T1 equilibrations effects. Next, the middle slice was used as the reference slice for slice time correction and motion correction realignment. Following this, the corrected images were coregistered to their respective T1-weighted image, and segmented into grey matter, white matter, and cerebrospinal fluid tissue maps using the DARTEL algorithm. Then, nuisance covariates regression, consisting of Friston 24 head-motion parameters, mean white matter and cerebrospinal fluid, and linear detrending was carried out. Global signal regression was also carried out to maximize the associations between functional connectivity and behavioral variables (Li et al., 2019). To further remove the effects of head motion, scrubbing was carried out on volumes with framewise displacement ($FD_{Jenkinson}$) > 0.2mm (Yan et al., 2013). Additionally, participants with excessive head motion, as operationalized by having a mean $FD_{Jenkinson}$ > 0.2mm, were excluded. Next, the images were normalized by DARTEL to MNI space with a voxel size of $3 \times 3 \times 3$ mm^3 and smoothed using a 4mm FWHM kernel. A band-pass filter of 0.01 to 0.1Hz was applied to the signal to remove the physiological high-frequency physiological noise and low-frequency drift.

For the network construction, the brainnetome atlas (Fan et al., 2016) was used to parcellate the whole brain into 246 anatomical regions corresponding to the nodes of the network. Previous research has shown rsFC connectivity matrices derived from partial correlations with L2 regularization tend to produce better predictions than connectivity matrices derived from Pearson correlation (Wu et al., 2021). Hence, prior to training the rsFC model, we converted the resting state ROI time-series data into partial correlation matrices with L2 regularization using the FSLNets' nets_netmats function (http://fsl.fmrib.ox.ac.uk/fsl/fslwiki/FSLNets).

The preprocessing of the diffusion images, tractography, and construction of the structural connectome were carried out using MRtrix3 (Tournier et al., 2019). Briefly, MP-PCA denoising (Veraart et al., 2016) and removal of Gibbs ringing artifacts (Kellner et al., 2016) were carried out on the raw images. Subsequently, they were corrected for motion, eddy currents and susceptibility-induced distortion using the inhomogeneity field maps obtained previously. Following this, bias field correction (Tustison et al., 2010) was carried out.

Next, the GM, WM, and CSF response functions were obtained using the Dhollander (Dhollander and Connelly, 2016) algorithm which are in turn used for estimating fiber orientation distributions (FOD) in the WM, GM and CSF tissues from diffusion data using spherical deconvolution. Then, anatomically-constrained tractography (Smith et al., 2012) was carried out using the WM FOD. This involved the prior preparation of a GM mask from the segmentation of the subject's T1 structural image using FSL FAST, and then using this mask to seed streamlines.

The AAL-90 atlas (Tzourio-Mazoyer et al., 2002) was used to parcellate the whole brain. For each subject, the AAL-90 template was first warped to the subject's native DTI space to obtain the transformations. Then, the warped template was overlaid onto the subject's diffusion tensors for visual inspection of the alignment. The transformations obtained previously were then applied to warp the AAL-90 atlas into the subject's native diffusion space. For the network construction in the subject's native diffusion space, the nodes i and j were thought to be connected by an edge ($e_{ij} = [i, j]$), if at least one reconstructed streamline was found with its two endpoints located within the two nodes, respectively. The edges in the connectivity matrix for each participant were operationalized as the number of streamlines connecting between each pair of regions. Finally, the thresholded matrices were normalized using the Brain Connectivity Toolbox (Rubinov and Sporns, 2010) within MATLAB.

2.6 Statistical analysis

To derive the brain- and cognitive-age prediction models, we trained ridge regression models separately on the five modalities of predictors (i.e., SC, rsFC, CT, subGM, and cognitive test scores) to predict participant's age using the Matlab function 'fitrlinear', within the ADNI dataset. Briefly, we first identified the optimal lambda parameters for the ridge regression models by testing 50 logarithmically-spaced values ranging from 10^{-5} to 10^{-2} in a 5-fold cross-validation (CV) paradigm. In order to minimize overfitting, we selected the largest lambda value that has a mean squared error (MSE) within one standard error of the minimum MSE (Gao et al., 2019). Then we repeated the ridge regression on the full ADNI sample using the selected lambda value to obtain the full-sample ridge regression loadings. Given that the optimal lambda value obtained in the 5-fold CV would vary depending on how participants were shuffled into the five folds, we repeated this process 1,000 times, with participants randomly shuffled into the folds each time. After which, the ridge regression loadings obtained from the full ADNI sample at the end of each iteration were averaged across the 1,000 iterations and these averaged loadings consequently constitute our brain-age (four independent models: SC, rsFC, CT, and subGM) and cognitive-age prediction models.

Next, we also constructed a stacked brain-age model, making use of all four brain modalities. First, we used the ADNI-derived brain-age models (all four modalities) to predict age within the ADNI sample, thus obtaining four sets of age predictions. These four sets of age predictions were then entered as input features into a random forest prediction model to predict participant's age within the ADNI sample. The hyperparameters for this stacked model were tuned automatically via another 5-fold CV using the 'OptimizeHyperparameters','auto' option within the 'fitrensemble' function in Matlab. To

quantify the contribution of the different modalities in predicting age, we estimated their prediction importance values.

Consequently, we would have generated five brain-age (i.e. SC, rsFC, CT, subGM, and the stacked model) and one cognitive-age prediction models. These five models were then applied to the SG participant's data to generate age predictions for each model. For each of these models, we assessed the accuracy of these predictions via the root mean square error (RMSE), mean absolute error (MAE), and correlation (Pearson's and Spearman's) between the predicted age and actual age. For every subject, we also computed the discrepancy in predictions (i.e., predicted age - actual age). Then we assessed the associations between these gaps and TL via Pearson's correlations. The age gaps were also compared across modalities using repeated measures analysis of variance (ANOVA). Statistical significance was set at $p<.05$. These analyses were carried out in MATLAB (R2021a) and R 4.0.2. The Matlab and R code for executing the analyses and generating the figures, as well as the preprocessed ADNI data are available at https://osf.io/vkejr/.

3. Results

3.1 Characteristics of age-prediction models

The ridge regression coefficients of the cognitive-age prediction model obtained across 1,000 permuted iterations (see figure 1) suggest that the cognitive age-prediction model was largely driven by Total learning, TMT-A, and TMT-B scores. Moving on to the brain-age prediction models, the age-related profiles of SC and rsFC are shown in figure 2c and d. In general, most of the SC connections were negatively associated with increasing age, while frontal-subcortical and subcortical-limbic connections were strengthen with age. In terms of rsFC, the patterns of connectivity were relatively mixed— different sets of connections were weakened and strengthened in relation to increasing age. Next, the age-related cortical profile is shown in figure 2a. In general, there was a mixture of negative and positive loadings, with the former clustered around superior and medial regions of the brain. The age-related subGM profile is shown in figure 2b. All of the subGM regions were negatively loaded, with the largest (absolute) loadings assigned to the bilateral thalamus. Finally, the proportion of predictor importance in the stacked random forest model is shown in figure 2e; the rsFC modality was associated with the largest predictor importance in the random forest model.

3.2 Predictive ability of age-prediction models

We applied ADNI-derived prediction models to the ADNI and SG datasets, and computed their prediction metrics (see figure 3). In terms of the precision (i.e., MAE and RMSE) of age prediction in the SG dataset, the CT and subGM models similarly outperformed the other models, whereas the cognitive model fared the worst. Nevertheless, in terms of the correlation between actual and predicted age in the SG dataset, the cognitive model performed the best, while the rsFC model fared the worst.

3.3 Age gaps and telomere length

The repeated measures ANOVA revealed significant differences between the age-gaps derived from the different age-prediction models (see figure 4). The results of the post-hoc tukey's tests suggest that participants' cognitive age was significantly 'older' than their brain-age estimates from the SC and rsFC models ($ps<.001$), their CT-ages were significantly 'older' than their SC- and rsFC ages ($ps\leq.0330$), and their subGM-ages were significantly older than their SC-ages ($p=.004$).

Given that demographical variables such as age, sex, and years of education were likely to confound these associations, we also performed partial correlation tests controlling for these variables. The partial correlation analyses suggest that the age gaps in the rsFC, CT, and stacked model were significantly and negatively correlated with telomere length (see figure 5). If we were to apply a bonferroni correction for the six sets of correlation analyses, only the partial r from the rsFC was statistically significant. On related note, TL was not significantly correlated with age ($r= -.09$, $p=.366$).

3.4 Supplementary analyses

We repeated all analyses involving the rsFC model, by using the conventional correlation instead of partial correlation rsFC matrices as input features. These results are presented in table S1. Generally, the correlation rsFC matrices produced a model that was slighty more overfitted to the ADNI dataset. This model's produced slightly more accurate age predictions in the ADNI dataset. Not surprisingly, it produced slightly less accurate predictions in the SG sample. Nevertheless, its age-gaps remained significantly correlated with TL, after controlling for age, sex, and years of education

4. Discussion

The current study tested the hypothesis that telomere shortening is linked to older brain and cognitive age gaps. We trained brain-age and cognitive-age prediction models using the ADNI dataset and applied these models to the SG dataset. Our results showed that these age-prediction models were fairly generalizable to the SG dataset; the obtained MAEs were in line with previous findings (Cole and Franke, 2017). Then we correlated the predicted-actual age gaps in each age prediction model with TL. The findings suggested that the predicted-actual age gaps from the cognitive-age model were not significantly correlated with TL, whereas the predicted-actual age gaps obtained from three brain age models were significantly and negatively correlated with TL. In particular, predicted-actual age gaps from the rsFC model showed the highest correlation with TL. Overall, these results suggest telomere shortening is significantly associated with 'older' brain age but not cognitive age.

Using the brain-age prediction approach, we provided novel evidence to show that telomere shortening is linked to 'older' brain age gaps in multiple modalities. It is interesting to note that rsFC brain age gaps are most strongly linked to telomere shortening. These gaps indirectly measure the deviations in the functional connectome in the SG sample from the ADNI sample. To this end, one can infer that telomere shortening is linked to changes in FC. Notwithstanding the cross-sectional nature of this study, which precludes the causal

inferences between telomere shortening and FC changes, we speculate such causal effects can possibly exist in both directions. First, the telomere-associated cellular senescence could have directly led to brain aging (Ain et al., 2018). Alternatively, age-related FC changes in the brain could have resulted in less self-restraint and inhibition (Tsvetanov et al., 2018), and subsequently influencing health-related behaviors. For instance, this could mean more frequent consumption of alcohol and tobacco, or unrestraint eating. These unhealthy behaviors would in turn shorten TL (Puterman et al., 2015).

Relatedly, we observed that the age gaps derived from the structural domains, especially SC, appeared to be less strongly implicated. The relatively different results in the rsFC and SC modalities are not unusual. Although rsFC and SC are related to each other, they are not very strongly coupled. Strong rsFC can thrive in the absence of strong SC since rsFC can rely on indirect structural connections (Damoiseaux, 2017). Furthermore, SC is likely to be more resilient to aging in general. Unlike rsFC networks, SC networks appear to be held together by a consistent set of highly connected and central hubs which remain mostly unchanged across the lifespan (Betzel, et al., 2014), thus ensuring the age-related stability in the SC network topography. Hence, the brain-aging trajectories in the rsFC and SC modalities are likely to diverge to some extent. Contrary to our hypothesis, the cognitive-chronological age gaps were not significantly associated with TL. In fact, these gaps were positively related (though not significantly) to TL, counterintuitively suggesting that telomere shortening was associated with ‘younger’ cognitive functions. This may not be unusual, as there were a handful of studies that showed that shorter TLs were associated with better cognitive functions (Harris et al., 2006; Lee et al., 2017; Liu et al., 2016; Mahoney et al., 2019; Wikgren et al., 2012). Furthermore, it was shown that this counterintuitive increase in cognitive functioning was predicted by telomere-shortening associated SC changes (Yu et al., 2020).

Our multimodal brain-age prediction models were largely consistent with previous research in showing that aging is associated with disrupted structural connections (Betzel et al., 2014) and significant cortical and subcortical GM atrophy (Oh et al., 2014). Amazingly, these ADNI-derived models generalized relatively well to the SG sample despite the different socio-demographics and MRI acquisition protocols in both samples— which is a further testament to the robustness of the brain-age prediction models. Nevertheless, the age-related rsFC profile obtained from the ADNI dataset did not appear to be consistent with previous research in showing an age-related decrease in within-network and increase in between-network connectivity (Damoiseaux, 2017; Zonneveld et al., 2019). Instead, our results suggested the opposite— increased within-network and decreased between-network connectivity. Such an atypical age-related rsFC profile is likely to be the consequence of using partial correlation, as opposed to the conventional correlation rsFC matrices as input features. As Wu et al. (2021) explained, this partial correlation approach removes the shared variance across regions, consequently, the pattern of brain connectivity between regions will be significantly distorted. Although partial correlation matrices would improve the model’s prediction performance, the connectivity profiles obtained from these matrices may not be as interpretable as those of correlation matrices.

On average, we see that the SG sample, consisting of individuals with MCI, had cognitive ages that were older than their chronological ages; this would be largely expected in light of the 'objective cognitive impairment' criterion of MCI. Furthermore, education levels were much lower in the SG sample than in the ADNI sample. Given that education constitutes a significant component of cognitive reserve and is strongly associated with cognitive functions (Whalley et al., 2004), the ADNI-derived cognitive age model is likely to overestimate the cognitive age in the SG sample. Next, our results also provided a rare opportunity to compare the pace of aging in the different brain modalities. We showed that cortical age gaps are the 'oldest' compared to those of other brain modalities in our MCI sample. Nevertheless, we imagine these results would be largely dependent on the etiology of MCI. For instance, we would expect individuals with MCI due to AD to undergo more rapid subcortical aging as compared to AD-unrelated MCI cases (Yi et al., 2016). In our sample of MCI subjects, the older cortical age gaps may hint at possible vascular-related etiologies (Lee et al., 2018).

Our findings present some important implications for brain-age predictions in general. The significant associations between brain-chronological age gaps and TL are a much-needed validation for brain age predictions in general. These brain age metrics can be used as indices of general brain health (Cole and Franke, 2017) with relative ease. Once a brain-age prediction model has been set up and adequately validated, it can be applied to patients' MRI scans to obtain their brain-age via largely automated procedures—requiring only very minimal technical expertise. Brain-age is also fairly simple to interpret and can be easily communicated to and understood by patients, unlike the more technical concepts of atrophy, lesions, or brain connectivity. Additionally, our results suggest that brain-age is largely influenced by patterns of rsFC. Given that rsFC is highly susceptible to experience-dependent plasticity (Kelly and Castellanos, 2014), this would open up a whole range of possibilities in using lifestyle or behavioral interventions to 'reverse' brain aging to improve brain health in general.

The current findings are subjected to two limitations. First, due to the small number of common cognitive tests used in both datasets, we may not have an adequate number of predictors in our cognitive-age model nor were we able to cover the different cognitive domains comprehensively. Second, although the age prediction models had generally demonstrated satisfactory levels of generalizability, it is likely that this generalizability could be higher if the MRI acquisition parameters were identical in both datasets. Third, the differences between the ADNI and SG samples in terms of education levels meant that the brain/cognitive age gap could not be entirely accounted for by accelerated brain aging/degeneration, but could also result from education-related factors implicating brain aging. Fourth, the use of the MCI-only sample in this study meant that these results cannot be generalized to or interpreted within the context of normal aging. It is likely that some disease-related factors, such that those relating to AD or cerebrovascular disease, might have accelerated brain aging and led to telomere shortening; consequently, significant correlations between brain aging and TL could be observed. Speculatively, in the absence of such disease-related factors, such correlations is less likely to be observed.

Verification

We verify that the work described has not been published previously, that it is not under consideration for publication elsewhere, that its publication is approved by all authors and tacitly or explicitly by the responsible authorities where the work was carried out, and that, if accepted, it will not be published elsewhere in the same form, in English or in any other language, including electronically without the written consent of the copyright-holder

Supplementary Material

Refer to Web version on PubMed Central for supplementary material.

Acknowledgments

The authors would like to thank Mengxia Gao for her assistance in the preprocessing of the ADNI dataset. This work was supported by Research Donations from Kwan Im Thong Hood Cho Temple and Lee Kim Tah Holdings Pte Ltd, under the Mind Science Centre, Department of Psychological Medicine, National University of Singapore. Junhong Yu is supported by the Nanyang Assistant Professorship (Award no. 021080-00001). The work was supported by a grant from the Singapore Ministry of Education Tier 2 (MOE-T2EP30120-0016) to A.P.K. The ADNI data collection and sharing was funded by the ADNI (National Institutes of Health Grant U01 AG024904) and DOD ADNI (Department of Defense award number W81XWH-12-2-0012). ADNI is funded by the National Institute on Aging, the National Institute of Biomedical Imaging and Bioengineering, and through generous contributions from the following: AbbVie, Alzheimer's Association; Alzheimer's Drug Discovery Foundation; Araclon Biotech; BioClinica, Inc.; Biogen; Bristol-Myers Squibb Company; CereSpir, Inc.; Cogstate; Eisai Inc.; Elan Pharmaceuticals, Inc.; Eli Lilly and Company; EuroImmun; F. Hoffmann-La Roche Ltd and its affiliated company Genentech, Inc.; Fujirebio; GE Healthcare; IXICO Ltd.; Janssen Alzheimer Immunotherapy Research & Development, LLC.; Johnson & Johnson Pharmaceutical Research & Development LLC.; Lumosity; Lundbeck; Merck & Co., Inc.; Meso Scale Diagnostics, LLC.; NeuroRx Research; Neurotrack Technologies; Novartis Pharmaceuticals Corporation; Pfizer Inc.; Piramal Imaging; Servier; Takeda Pharmaceutical Company; and Transition Therapeutics. The Canadian Institutes of Health Research is providing funds to support ADNI clinical sites in Canada. Private sector contributions are facilitated by the Foundation for the National Institutes of Health (www.fnih.org). The grantee organization is the Northern California Institute for Research and Education, and the study is coordinated by the Alzheimer's Therapeutic Research Institute at the University of Southern California. ADNI data are disseminated by the Laboratory for Neuro Imaging at the University of Southern California

References

Ain Q, Schmeer C, Penndorf D, Fischer M, Bondeva T, Förster M, Haenold R, Witte OW, Kretz A, 2018. Cell cycle-dependent and -independent telomere shortening accompanies murine brain aging. Aging (Albany. NY). 10, 3397–3420. 10.18632/aging.101655 [PubMed: 30472697]

Ashburner J, 2007. A fast diffeomorphic image registration algorithm. Neuroimage 38, 95–113. [PubMed: 17761438]

Badhwar AP, Tam A, Dansereau C, Orban P, Hoffstaedter F, Bellec P, 2017. Resting-state network dysfunction in Alzheimer's disease: A systematic review and meta-analysis. Alzheimer's Dement. Diagnosis, Assess. Dis. Monit 8, 73–85. 10.1016/j.dadm.2017.03.007

Betzel RF, Byrge L, He Y, Goñi J, Zuo XN, Sporns O, 2014. Changes in structural and functional connectivity among resting-state networks across the human lifespan. Neuroimage 102, 345–357. 10.1016/j.neuroimage.2014.07.067 [PubMed: 25109530]

Blair RJR, Zhang R, 2020. Recent neuro-imaging findings with respect to conduct disorder, callous-unemotional traits and psychopathy. Curr. Opin. Psychiatry 33, 45–50. 10.1097/YCO.0000000000000559 [PubMed: 31725420]

Brown LL, Zhang YS, Mitchell C, Ailshire J, 2018. Does Telomere Length Indicate Biological, Physical, and Cognitive Health Among Older Adults? Evidence from the Health and Retirement Study. Journals Gerontol. Ser. A 73, 1626–1632. 10.1093/gerona/gly001

Castaneda AE, Tuulio-Henriksson A, Marttunen M, Suvisaari J, Lönnqvist J, 2008. A review on cognitive impairments in depressive and anxiety disorders with a focus on young adults. J. Affect. Disord 106, 1–27. [PubMed: 17707915]

Chew KA, Chong EJY, Chen CLH, Xu X, 2020. Psychometric Properties of the National Institute of Neurological Disorders and Stroke and Canadian Stroke Network Neuropsychological Battery in an Asian Older Adult Sample. J. Am. Med. Dir. Assoc 21, 879–883. [PubMed: 32444287]

Cole JH, Franke K, 2017. Predicting age using neuroimaging: innovative brain ageing biomarkers. Trends Neurosci. 40, 681–690. [PubMed: 29074032]

D'Elia L, Satz P, 1996. Color trails test. Psychological Assessment Resources, Odessa, FL.

Dahnke R, Yotter RA, Gaser C, 2013. Cortical thickness and central surface estimation. Neuroimage 65, 336–348. [PubMed: 23041529]

Damoiseaux JS, 2017. Effects of aging on functional and structural brain connectivity. Neuroimage 160, 32–40. 10.1016/j.neuroimage.2017.01.077 [PubMed: 28159687]

Destrieux C, Fischl B, Dale A, Halgren E, 2010. Automatic parcellation of human cortical gyri and sulci using standard anatomical nomenclature. Neuroimage 53, 1–15. [PubMed: 20547229]

Dhollander T, Connelly A, 2016. A novel iterative approach to reap the benefits of multi-tissue CSD from just single-shell (+b=0) diffusion MRI data.

Elliott ML, Belsky DW, Knodt AR et al. Brain-age in midlife is associated with accelerated biological aging and cognitive decline in a longitudinal birth cohort. Mol Psychiatry 26, 3829–3838 2021. 10.1038/s41380-019-0626-7 [PubMed: 31822815]

Fan L, Li H, Zhuo J, Zhang Y, Wang J, Chen L, Yang Z, Chu C, Xie S, Laird AR, 2016. The human brainnetome atlas: a new brain atlas based on connectional architecture. Cereb. cortex 26, 3508–3526. [PubMed: 27230218]

Feng L, Chong MS, Lim WS, Ng TP, 2012. The Modified Mini-Mental State Examination test: normative data for Singapore Chinese older adults and its performance in detecting early cognitive impairment. Singapore Med J 53, 458–462. [PubMed: 22815014]

Folstein MF, Folstein SE, McHugh PR, 1975. "Mini-mental state". A practical method for grading the cognitive state of patients for the clinician. J. Psychiatr. Res 12, 189–198. [PubMed: 1202204]

Gao S, Greene AS, Constable RT, Scheinost D, 2019. Combining multiple connectomes improves predictive modeling of phenotypic measures. Neuroimage 201, 116038. https://doi.org/10.1016/j.neuroimage.2019.116038 [PubMed: 31336188]

Giardini MA, Segatto M, da Silva MS, Nunes VS, Cano MIN, 2014. Telomere and telomerase biology. Prog. Mol. Biol. Transl. Sci 125, 1–40. 10.1016/B978-0-12-397898-1.00001-3 [PubMed: 24993696]

Gohring J, Fulcher N, Jacak J, Riha K, 2014. TeloTool: a new tool for telomere length measurement from terminal restriction fragment analysis with improved probe intensity correction. Nucleic Acids Res. 42, e21. 10.1093/nar/gkt1315 [PubMed: 24366880]

Hägg S, Zhan Y, Karlsson R, Gerritsen L, Ploner A, van der Lee SJ, Broer L, Deelen J, Marioni RE, Wong A, Lundquist A, Zhu G, Hansell NK, Sillanpää E, Fedko IO, Amin NA, Beekman M, de Craen AJM, Degerman S, Harris SE, Kan K-J, Martin-Ruiz CM, Montgomery GW, Adolfsson AN, Reynolds CA, Samani NJ, Suchiman HED, Viljanen A, von Zglinicki T, Wright MJ, Hottenga J-J, Boomsma DI, Rantanen T, Kaprio JA, Nyholt DR, Martin NG, Nyberg L, Adolfsson R, Kuh D, Starr JM, Deary IJ, Slagboom PE, van Duijn CM, Codd V, Pedersen NL, Group NCW, Consortium, for the E., 2017. Short telomere length is associated with impaired cognitive performance in European ancestry cohorts. Transl. Psychiatry 7, e1100–e1100. 10.1038/tp.2017.73 [PubMed: 28418400]

Harris SE, Deary IJ, MacIntyre A, Lamb KJ, Radhakrishnan K, Starr JM, Whalley LJ, Shiels PG, 2006. The association between telomere length, physical health, cognitive ageing, and mortality in non-demented older people. Neurosci. Lett 406, 260–264. 10.1016/j.neulet.2006.07.055 [PubMed: 16919874]

Jacobs EG, Epel ES, Lin J, Blackburn EH, Rasgon NL, 2014. Relationship between leukocyte telomere length, telomerase activity, and hippocampal volume in early aging. JAMA Neurol. 71, 921–923. [PubMed: 25023551]

Kellner E, Dhital B, Kiselev VG, Reisert M, 2016. Gibbs-ringing artifact removal based on local subvoxel-shifts. Magn. Reson. Med 76, 1574–1581. 10.1002/mrm.26054 [PubMed: 26745823]

Kelly C, Castellanos FX, 2014. Strengthening Connections: Functional Connectivity and Brain Plasticity. Neuropsychol. Rev 24, 63–76. 10.1007/s11065-014-9252-y [PubMed: 24496903]

King KS, Kozlitina J, Rosenberg RN, Peshock RM, McColl RW, Garcia CK, 2014. Effect of Leukocyte Telomere Length on Total and Regional Brain Volumes in a Large Population-Based Cohort. JAMA Neurol. 71, 1247–1254. 10.1001/jamaneurol.2014.1926 [PubMed: 25090243]

Lee J-Y, Kim J-H, Lee D-C, 2017. Combined Impact of Telomere Length and Mitochondrial DNA Copy Number on Cognitive Function in Community-Dwelling Very Old Adults. Dement. Geriatr. Cogn. Disord 44, 232–243. 10.1159/000480427 [PubMed: 28982094]

Lee J, Seo SW, Yang J-J, Jang YK, Lee JS, Kim YJ, Chin J, Lee JM, Kim ST, Lee K-H, Lee JH, Kim JS, Kim S, Yoo H, Lee AY, Na DL, Kim HJ, 2018. Longitudinal cortical thinning and cognitive decline in patients with early- versus late-stage subcortical vascular mild cognitive impairment. Eur. J. Neurol 25, 326–333. 10.1111/ene.13500 [PubMed: 29082576]

Lee TMC, Chan CCH, 2000. Are Trail Making and Color Trails Tests of Equivalent Constructs? J. Clin. Exp. Neuropsychol 22, 529–534. 10.1076/1380-3395(200008)22:4;1-0;FT529 [PubMed: 10923062]

Lee TMC, Cheung CCY, Chan JKP, Chan CCH, 2000. Trail making across languages. J. Clin. Exp. Neuropsychol 22, 772–778. [PubMed: 11320435]

Leibel DK, Shaked D, Beatty Moody DL, Liu HB, Weng N, Evans MK, Zonderman AB, Waldstein SR, 2020. Telomere length and cognitive function: Differential patterns across sociodemographic groups. Neuropsychology. 10.1037/neu0000601

Li J, Kong R, Liégeois R, Orban C, Tan Y, Sun N, Holmes AJ, Sabuncu MR, Ge T, Yeo BTT, 2019. Global signal regression strengthens association between resting-state functional connectivity and behavior. Neuroimage 196, 126–141. 10.1016/j.neuroimage.2019.04.016 [PubMed: 30974241]

Liem F, Varoquaux G, Kynast J, Beyer F, Kharabian Masouleh S, Huntenburg JM, Lampe L, Rahim M, Abraham A, Craddock RC, Riedel-Heller S, Luck T, Loeffler M, Schroeter ML, Witte AV, Villringer A, Margulies DS, 2017. Predicting brain-age from multimodal imaging data captures cognitive impairment. Neuroimage 148, 179–188. https://doi.org/10.1016/j.neuroimage.2016.11.005 [PubMed: 27890805]

Liu M, Huo YR, Wang Junwei, Wang C, Liu Shuling, Liu Shuai, Wang Jinhuan, Ji Y, 2016. Telomere Shortening in Alzheimer's Disease Patients. Ann. Clin. Lab. Sci 46, 260–265. [PubMed: 27312549]

Löwe LC, Gaser C, Franke K, Initiative, for the A.D.N., 2016. The Effect of the APOE Genotype on Individual BrainAGE in Normal Aging, Mild Cognitive Impairment, and Alzheimer's Disease. PLoS One 11, e0157514. [PubMed: 27410431]

Ma F, Lv X, Du Y, Chen H, Liu S, Zhao J, Gao Y, An P, Zhou X, Song A, Sun C, Wang G, Ji Y, Wang X, Xu W, Huang G, 2019. Association of Leukocyte Telomere Length with Mild Cognitive Impairment and Alzheimer's Disease: Role of Folate and Homocysteine. Dement. Geriatr. Cogn. Disord 48, 56–67. 10.1159/000501958 [PubMed: 31437841]

Mahoney ER, Dumitrescu L, Seto M, Nudelman KNH, Buckley RF, Gifford KA, Saykin AJ, Jefferson AJ, Hohman TJ, 2019. Telomere length associations with cognition depend on Alzheimer's disease biomarkers. Alzheimer's Dement. Transl. Res. Clin. Interv 5, 883–890. 10.1016/j.trci.2019.11.003

Minkova L, Habich A, Peter J, Kaller CP, Eickhoff SB, Klöppel S, 2017. Gray matter asymmetries in aging and neurodegeneration: A review and meta- analysis. Hum. Brain Mapp 38, 5890–5904. [PubMed: 28856766]

Njajou OT, Hsueh W-C, Blackburn EH, Newman AB, Wu S-H, Li R, Simonsick EM, Harris TM, Cummings SR, Cawthon RM, study, for the H.A.B.C., 2009. Association Between Telomere Length, Specific Causes of Death, and Years of Healthy Life in Health, Aging, and Body Composition, a Population-Based Cohort Study. Journals Gerontol. Ser. A 64A, 860–864. 10.1093/gerona/glp061

Oh H, Madison C, Villeneuve S, Markley C, Jagust WJ, 2014. Association of Gray Matter Atrophy with Age, β-Amyloid, and Cognition in Aging. Cereb. Cortex 24, 1609–1618. 10.1093/cercor/bht017 [PubMed: 23389995]

Petersen RC, 2004. Mild cognitive impairment as a diagnostic entity. J. Intern. Med 256, 183–194. 10.1111/j.1365-2796.2004.01388.x [PubMed: 15324362]

Powell TR, Dima D, Frangou S, Breen G, 2018. Telomere Length and Bipolar Disorder. Neuropsychopharmacology 43, 445–453. 10.1038/npp.2017.125 [PubMed: 28621334]

Puterman E, Lin J, Krauss J, Blackburn EH, Epel ES, 2015. Determinants of telomere attrition over 1 year in healthy older women: stress and health behaviors matter. Mol. Psychiatry 20, 529–535. 10.1038/mp.2014.70 [PubMed: 25070535]

Rane G, Koh W-P, Kanchi MM, Wang R, Yuan J-M, Wang X, 2015. Association Between Leukocyte Telomere Length and Plasma Homocysteine in a Singapore Chinese Population. Rejuvenation Res. 18, 203–210. 10.1089/rej.2014.1617 [PubMed: 25546508]

Redlich R, Opel N, Bürger C, Dohm K, Grotegerd D, Förster K, Zaremba D, Meinert S, Repple J, Enneking V, Leehr E, Böhnlein J, Winters L, Froböse N, Thrun S, Emtmann J, Heindel W, Kugel H, Arolt V, Romer G, Postert C, Dannlowski U, 2018. The Limbic System in Youth Depression: Brain Structural and Functional Alterations in Adolescent In-patients with Severe Depression. Neuropsychopharmacology 43, 546–554. 10.1038/npp.2017.246 [PubMed: 29039414]

Reitan RM, 1992. Trail Making Test: Manual for administration and scoring. Reitan Neuropsychology Laboratory, Odessa, FL.

Rey A, 1941. L'examen psychologique dans les cas d'enc{é}phalopathie traumatique.(Les problems.). Arch. Psychol. (Geneve)

Rubinov M, Sporns O, 2010. Complex network measures of brain connectivity: Uses and interpretations. Neuroimage 52, 1059–1069. https://doi.org/10.1016/j.neuroimage.2009.10.003 [PubMed: 19819337]

Shen JH, Shen Q, Yu H, Lai J-S, Beaumont JL, Zhang Z, Wang H, Kim SY, Chen C, Kwok T, Wang S-J, Lee DY, Harrison J, Cummings J, 2014. Validation of an Alzheimer's disease assessment battery in Asian participants with mild to moderate Alzheimer's disease. Am. J. Neurodegener. Dis 3, 158–169. [PubMed: 25628967]

Smith RE, Tournier J-D, Calamante F, Connelly A, 2012. Anatomically-constrained tractography: improved diffusion MRI streamlines tractography through effective use of anatomical information. Neuroimage 62, 1924–1938. 10.1016/j.neuroimage.2012.06.005 [PubMed: 22705374]

Staffaroni AM, Tosun D, Lin J, Elahi FM, Casaletto KB, Wynn MJ, Patel N, Neuhaus J, Walters SM, Epel ES, Blackburn EH, Kramer JH, 2018. Telomere attrition is associated with declines in medial temporal lobe volume and white matter microstructure in functionally independent older adults. Neurobiol. Aging 69, 68–75. 10.1016/j.neurobiolaging.2018.04.021 [PubMed: 29859365]

Tournier JD, Smith R, Raffelt D, Tabbara R, Dhollander T, Pietsch M, Christiaens D, Jeurissen B, Yeh CH, Connelly A, 2019. MRtrix3: A fast, flexible and open software framework for medical image processing and visualisation. Neuroimage 202, 116137. 10.1016/j.neuroimage.2019.116137 [PubMed: 31473352]

Tsvetanov KA, Ye Z, Hughes L, Samu D, Treder MS, Wolpe N, Tyler LK, Rowe JB, Neuroscience, for the C.C. for A. and, 2018. Activity and Connectivity Differences Underlying Inhibitory Control Across the Adult Life Span. J. Neurosci 38, 7887 LP – 7900. 10.1523/JNEUROSCI.2919-17.2018 [PubMed: 30049889]

Turner KJ, Vasu V, Griffin DK, 2019. Telomere Biology and Human Phenotype. Cells 8. 10.3390/cells8010073

Tustison NJ, Avants BB, Cook PA, Zheng Y, Egan A, Yushkevich PA, Gee JC, 2010. N4ITK: Improved N3 Bias Correction. IEEE Trans. Med. Imaging 29, 1310–1320. 10.1109/TMI.2010.2046908 [PubMed: 20378467]

Tzourio-Mazoyer N, Landeau B, Papathanassiou D, Crivello F, Etard O, Delcroix N, Mazoyer B, Joliot M, 2002. Automated Anatomical Labeling of Activations in SPM Using a Macroscopic Anatomical Parcellation of the MNI MRI Single-Subject Brain. Neuroimage 15, 273–289. https://doi.org/10.1006/nimg.2001.0978 [PubMed: 11771995]

Veraart J, Novikov DS, Christiaens D, Ades-aron B, Sijbers J, Fieremans E, 2016. Denoising of diffusion MRI using random matrix theory. Neuroimage 142, 394–406. https://doi.org/10.1016/j.neuroimage.2016.08.016 [PubMed: 27523449]

Whalley LJ, Deary IJ, Appleton CL, Starr JM, 2004. Cognitive reserve and the neurobiology of cognitive aging. Ageing Res. Rev 3, 369–382. [PubMed: 15541707]

Wikgren M, Karlsson T, Nilbrink T, Nordfjäll K, Hultdin J, Sleegers K, Van Broeckhoven C, Nyberg L, Roos G, Nilsson L-G, Adolfsson R, Norrback K-F, 2012. APOE ε4 is associated with longer telomeres, and longer telomeres among ε4 carriers predicts worse episodic memory. Neurobiol. Aging 33, 335–344. https://doi.org/10.1016/j.neurobiolaging.2010.03.004 [PubMed: 20395015]

Wu J, Eickhoff SB, Hoffstaedter F, Patil KR, Schwender H, Yeo BTT, Genon S, 2021. A Connectivity-Based Psychometric Prediction Framework for Brain–Behavior Relationship Studies. Cereb. Cortex 10.1093/cercor/bhab044

Yan C-G, Cheung B, Kelly C, Colcombe S, Craddock RC, Di Martino A, Li Q, Zuo X-N, Castellanos FX, Milham MP, 2013. A comprehensive assessment of regional variation in the impact of head micromovements on functional connectomics. Neuroimage 76, 183–201. https://doi.org/10.1016/j.neuroimage.2013.03.004 [PubMed: 23499792]

Yi H-A, Möller C, Dieleman N, Bouwman FH, Barkhof F, Scheltens P, van der Flier WM, Vrenken H, 2016. Relation between subcortical grey matter atrophy and conversion from mild cognitive impairment to Alzheimer's disease. J. Neurol. Neurosurg. & Psychiatry 87, 425 LP – 432. 10.1136/jnnp-2014-309105 [PubMed: 25904810]

Yotter Rachel Aine, Dahnke R, Thompson PM, Gaser C, 2011. Topological correction of brain surface meshes using spherical harmonics. Hum. Brain Mapp 32, 1109–1124. [PubMed: 20665722]

Yotter Rachel A, Thompson PM, Gaser C, 2011. Algorithms to improve the reparameterization of spherical mappings of brain surface meshes. J. Neuroimaging 21, e134–e147. [PubMed: 20412393]

Yu J, Kanchi MM, Rawtaer I, Feng L, Kumar AP, Kua E-H, Mahendran R, 2020. The functional and structural connectomes of telomere length and their association with cognition in mild cognitive impairment. Cortex 132, 29–40. https://doi.org/10.1016/j.cortex.2020.08.006 [PubMed: 32919107]

Yu J, Lam CLM, Lee TMC, 2017. White matter microstructural abnormalities in amnestic mild cognitive impairment: A meta-analysis of whole-brain and ROI-based studies. Neurosci. Biobehav. Rev 83, 405–416. 10.1016/j.neubiorev.2017.10.026 [PubMed: 29092777]

Yu J, Rawtaer I, Feng L, Fam J, Prem A, Cheah IK, Honer WG, Su W, Kun Y, Choo E, Heok E, Mahendran R, 2021a. Mindfulness intervention for mild cognitive impairment led to attention-related improvements and neuroplastic changes : Results from a 9-month randomized control trial. J. Psychiatr. Res 135, 203–211. 10.1016/j.jpsychires.2021.01.032 [PubMed: 33497874]

Yu J, Rawtaer I, Goh LG, Kumar AP, Feng L, Kua EH, Mahendran R, 2021b. The Art of Remediating Age-Related Cognitive Decline: Art Therapy Enhances Cognition and Increases Cortical Thickness in Mild Cognitive Impairment. J. Int. Neuropsychol. Soc 27, 79–88. 10.1017/S1355617720000697 [PubMed: 32762792]

Zhan Y, Clements MS, Roberts RO, Vassilaki M, Druliner BR, Boardman LA, Petersen RC, Reynolds CA, Pedersen NL, Hägg S, 2018. Association of telomere length with general cognitive trajectories: a meta-analysis of four prospective cohort studies. Neurobiol. Aging 69, 111–116. https://doi.org/10.1016/j.neurobiolaging.2018.05.004 [PubMed: 29870951]

Zhang J, Rane G, Dai X, Shanmugam MK, Arfuso F, Samy RP, Lai MKP, Kappei D, Kumar AP, Sethi G, 2016. Ageing and the telomere connection: An intimate relationship with inflammation. Ageing Res. Rev 25, 55–69. 10.1016/j.arr.2015.11.006 [PubMed: 26616852]

Zonneveld HI, Pruim RHR, Bos D, Vrooman HA, Muetzel RL, Hofman A, Rombouts SARB, van der Lugt A, Niessen WJ, Ikram MA, Vernooij MW, 2019. Patterns of functional connectivity in an aging population: The Rotterdam Study. Neuroimage 189, 432–444. https://doi.org/10.1016/j.neuroimage.2019.01.041 [PubMed: 30659958]

Highlights

- Chronological-age is best predicted by resting-state functional brain connectivity
- Shorter telomeres predict '**older**' brain-age and chronological-age discrepancies
- Shorter telomeres are more strongly linked to functional than structural brain aging

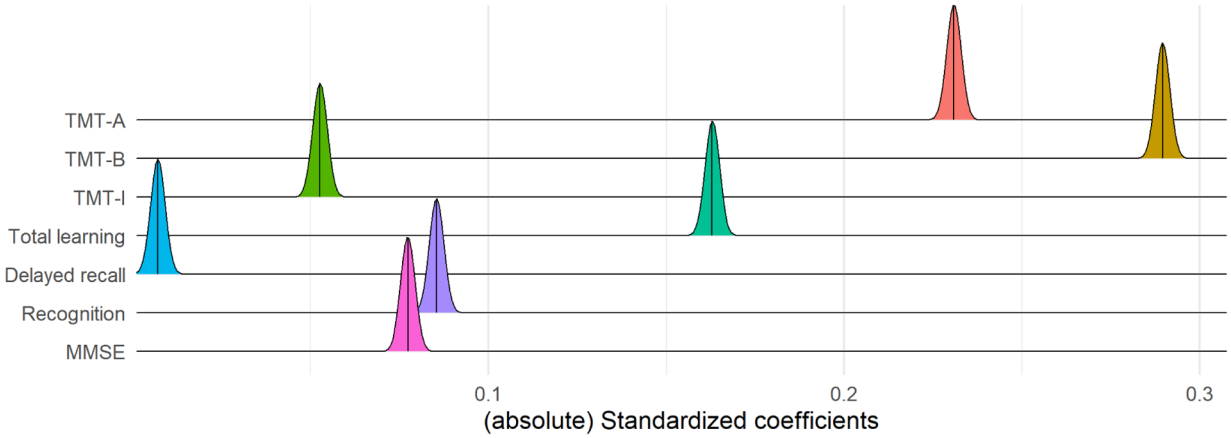

Figure 1.

Ridgeline plot showing the distribution of coefficients in the cognitive-age prediction model, across 1,000 permuted iterations within the ADNI sample. The vertical lines within the ridges represent their respective means. TMT= Trail Making Test; MMSE=Mini-Mental State Exam

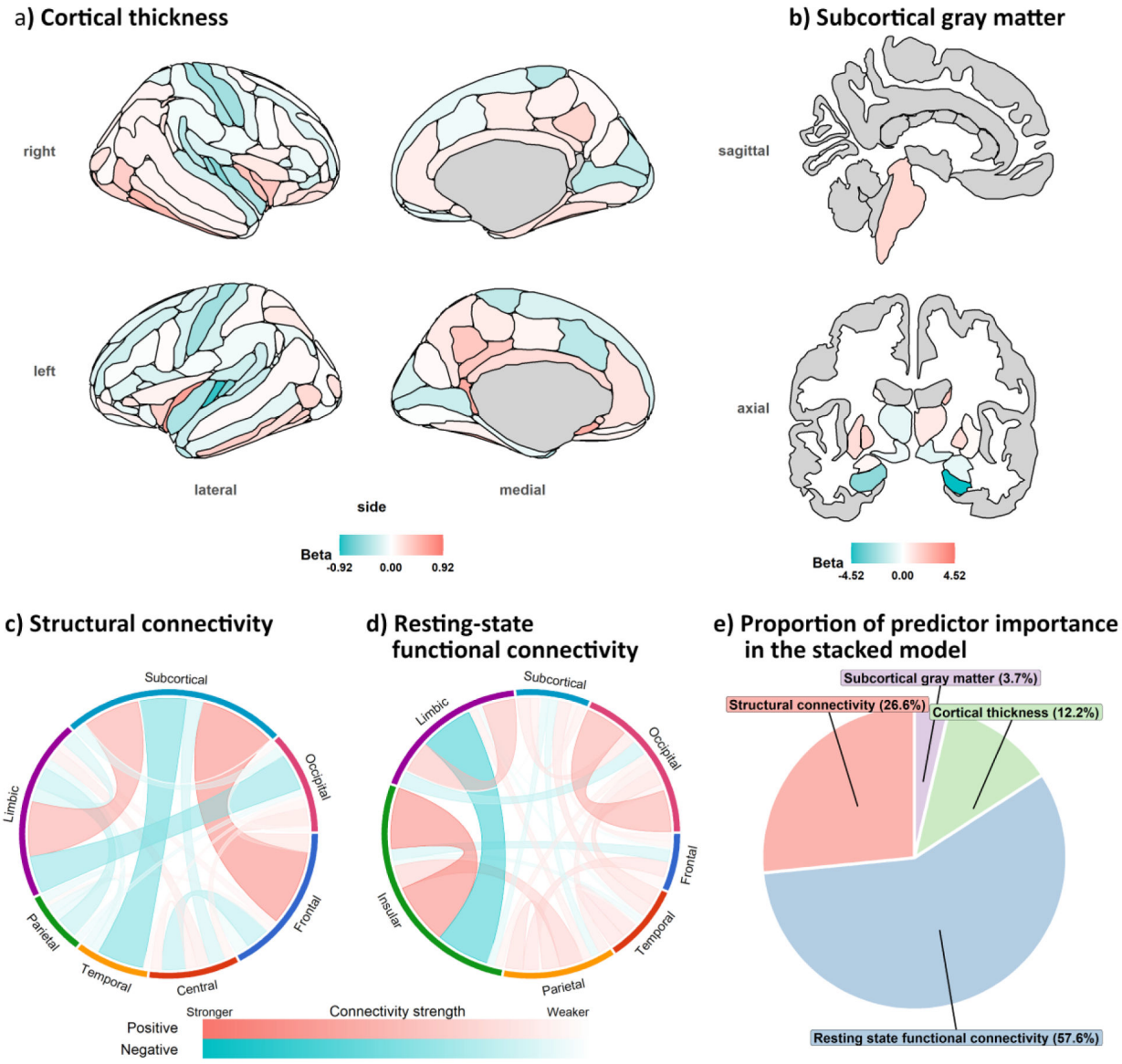

Figure 2.

Averaged ridge regression loadings across the 1000 permuted iterations in the a) cortical thickness b) subcortical gray matter, c) structural connectivity and d) resting state connectivity age prediction models. e) predictor importance in the stacked model. Note. the left and right nucleus accumbens regions which have the loadings of −0.29 and −0.33, respectively, could not be shown together with the other subcortical brain regions within the same sagittal and axial slice in b).

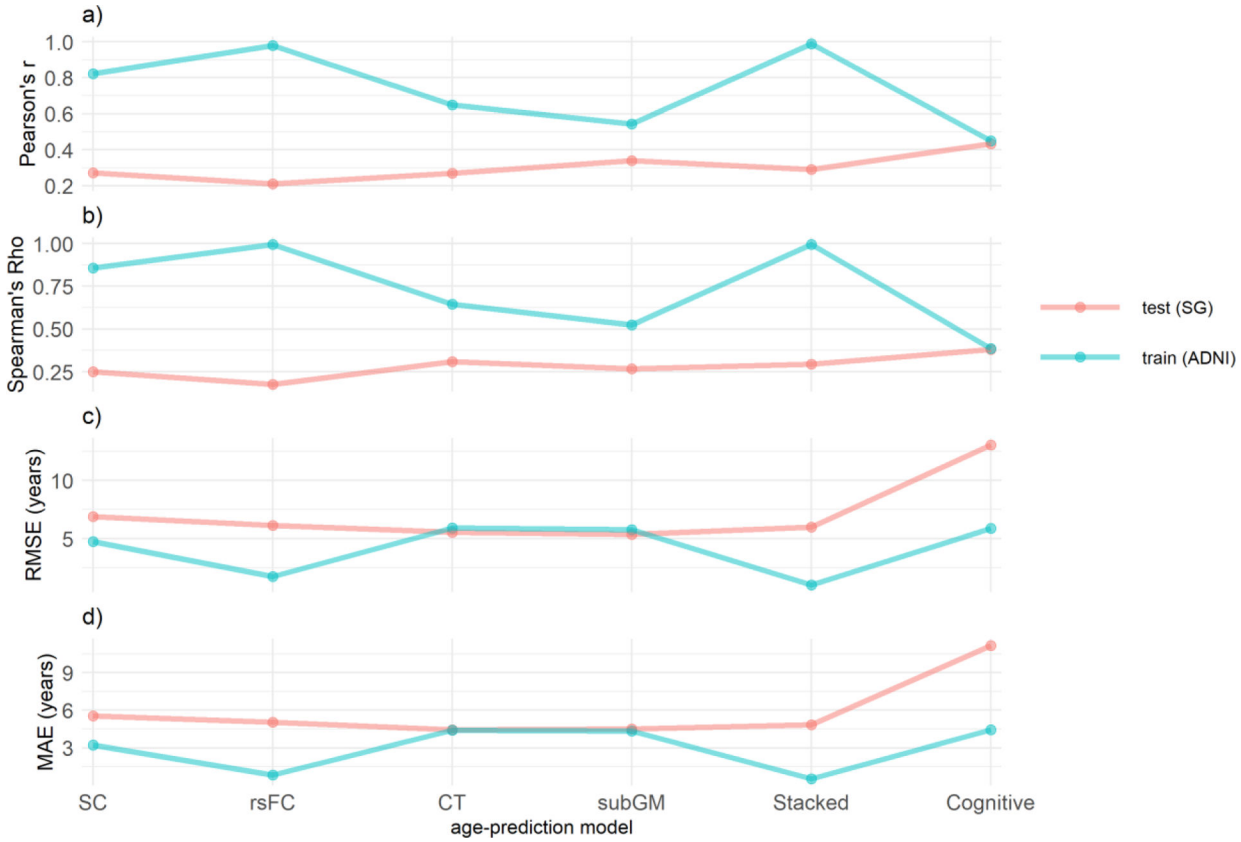

Figure 3.

Accuracy of age-prediction models as quantified by a) Pearson's r, b) Spearman's Rho, c) root mean square error and d) mean absolute error. SC= structural connectivity; rsFC = resting state functional connectivity; CT= cortical thickness; subGM= subcortical gray matter.

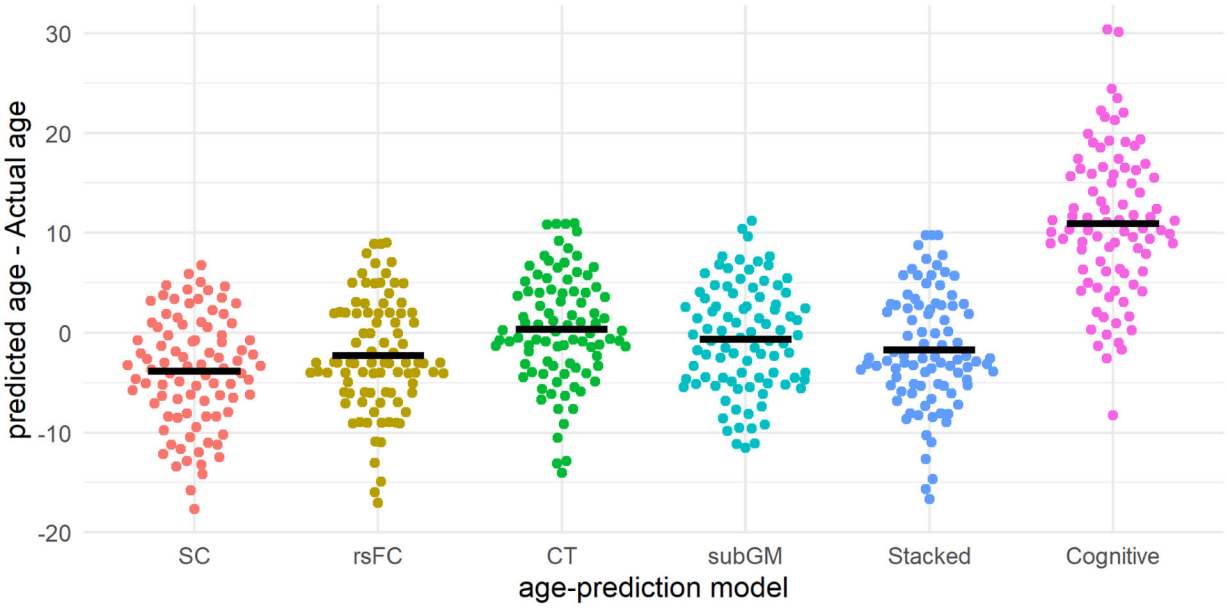

Figure 4.

Beehive plots showing the distribution of predict-actual age gaps across the different age-prediction models. The thick black lines represent the mean predict-actual age discrepancies in their respective age-prediction models. SC= structural connectivity; rsFC = resting state functional connectivity; CT= cortical thickness; subGM= subcortical gray.

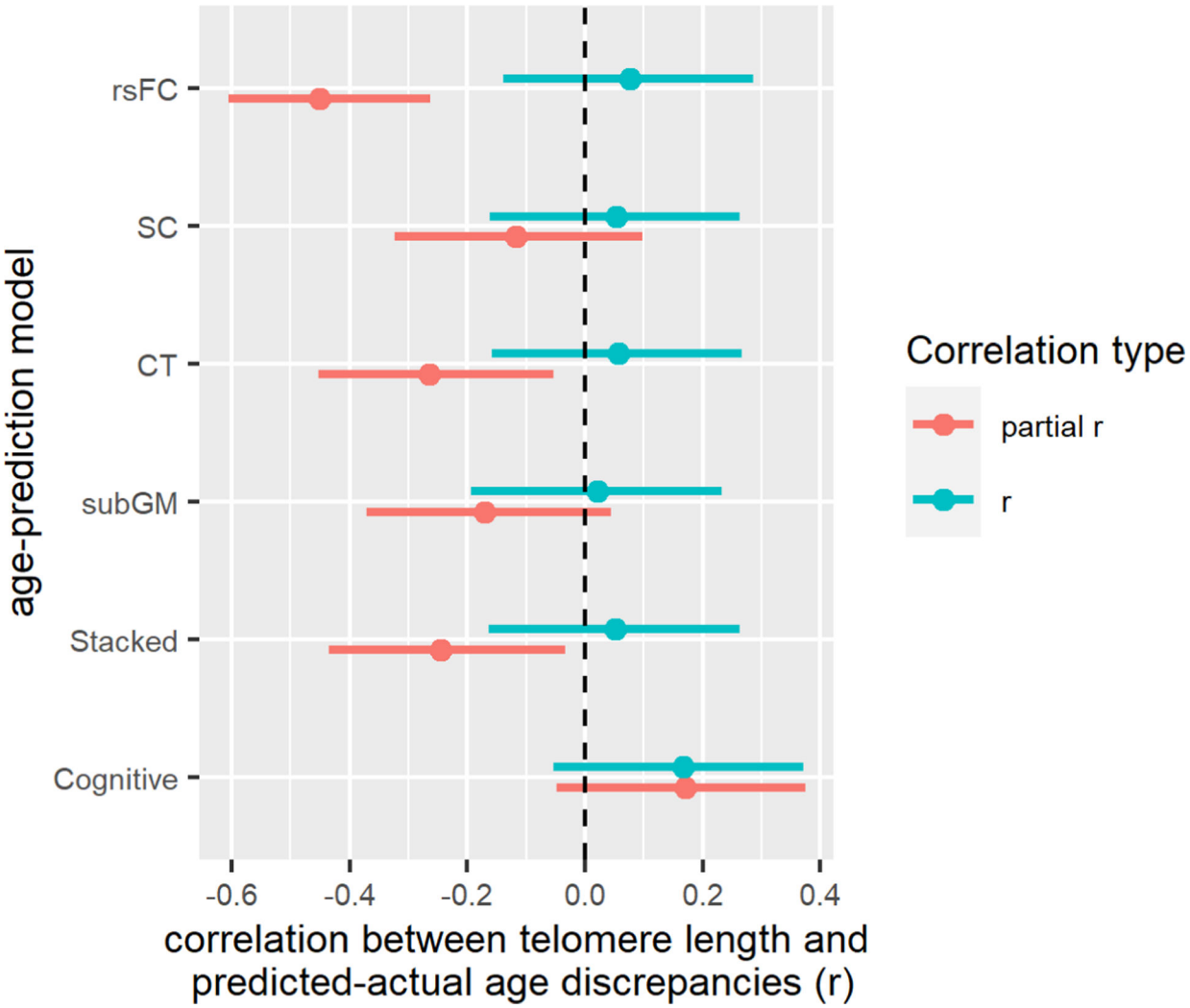

Figure 5.

Forest plots showing the correlations between telomere length and predicted-actual age gaps from the different age-prediction models. Note. 'partial r' is controlled for age, sex and years of education. The error bars represent the 95% confidence intervals of the correlation coefficients. SC= structural connectivity; rsFC = resting state functional connectivity; CT= cortical thickness; subGM= subcortical gray matter.

Table 1.

demographical characteristics of both groups of participants

Dataset	ADNI (N=196)	SG (N=91)
Mean age (SD)	70.7 (6.5)	71.3 (5.7)
% females	60%	76%
Mean years of education (SD)	16.9 (2.2)	5.1 (4.2)
Mean MMSE score (SD)	29.0 (1.1)	25.3 (3.3)

Note. SD= standard deviation; MMSE=mini-mental state examination.